Quaternary International 380-381 (2015) 314–326

Contents lists available at ScienceDirect

Quaternary International

journal homepage: www.elsevier.com/locate/quaint

Morphological evolution of the South Passage in the Changjiang (Yangtze River) estuary, China

Zhijun Dai [a,*], James T. Liu [b], Wei Wen [a]

[a] State Key Lab of Estuarine & Coastal Research, East China Normal University, Shanghai 20006, China
[b] Department of Oceanography, National Sun Yat-sen, Kaohsiung 80424, Taiwan

ARTICLE INFO

Article history:
Available online 7 March 2015

Keywords:
Estuarine morphology
Branching estuary
Shoal evolution
River runoff
River sediment load
EOF analysis

ABSTRACT

Estuarine morphology of the world's major large rivers have experienced great changes due to intensive anthropogenic activities and natural forcings, especially in the Changjiang Estuary located at the end of the longest river in Asia. This study focuses on morphological changes of the South Passage (SP), which is one of the 4 channels in the branching estuary at the mouth of the Changjiang (Yangtze River), China. A multivariate analysis technique of Empirical Orthogonal/Eigen Function (EOF) method was used to examine the major modes of change in the long-term (over 26 years) water-depth data. The results show that the morphological changes at the SP could be divided into two stages: between 1987 and 1997, the SP had a single stable channel with closure of a cross-channel. Between 1997 and 2012, SP displayed southeastward elongation of a spit into the main channel, and westward shoal incision by a cross-channel. The opening of the SP developed a two-channel morphology, which stabilized and showed infilling during 2003–2012. The average deposition rate was 10 cm/yr. In the past 30 years, the most dominant morphological changes of SP included the deposition around the upstream opening of the channel. The second most important pattern of morphological change was related to the downstream elongation, retreat, and lateral migration of the spit of the Jiangyanan Shoal, which resulted in the two-channel configuration of the SP. Additionally, these morphological changes were not triggered by the decline of the distal sediment source from the upstream, but due to the input of proximal sources of the shoal at the upstream opening of the SP and spill-over sediment from the North Passage via a short-cut-channel.

1. Introduction

Estuaries are located in the narrow zone of the land-sea boundary, which are valuable areas of both local and global importance. The morphology of estuaries is closely linked to estuarine assets such as natural location to ports (Van der Wegen and Roelvink, 2008). The morphological formation and evolution of estuaries is relatively gradual and has a typical decadal timescale. Small-scale sea-level fluctuations may trigger drastic changes (Dyer, 1997). However, in the last century the gradual development of many estuaries and adjacent area has been interrupted by human activities (Lane, 2004; Kao and Milliman, 2008; Evans, 2012; Gong et al., 2012; Li et al., 2012). Such practices include for example, damming of the river, construction of dikes and groins in the river mouth, and land reclamation (Chu et al., 2009; Syvitski et al., 2009; Dai and Lu, 2010; Evans, 2012).

The reduction of river load due to damming is the cause for risks of erosion and inundation in many estuaries and deltas in the world (Walling and Fang, 2003; Syvitski et al., 2005). A well-known example is the Nile delta. Because of the Aswan Dam, the erosion rate for the area around Rosetta Promontory was 10×10^6 m^3/y (Inman and Jenkins, 1984). Because of the construction of the dam at Adana, the nearby Seyhan delta in Turkey has the erosion rate of 1×10^6 m^3/y Gagliano et al. (1981) estimated the land loss around the mouth of the Mississippi was 102.1 km^2 in 1980, which was higher than those of 1987, 1946, and 1913 at 72.8, 40.9, and 17.4 km^2/y, respectively. Compared to the previous century, the Ebro River in Spain lost 99% of its load due to the constructions of dams and reservoirs (Gullén and Palanques, 1997). The Danube lost 35% of its load due to dam construction that led to the erosion at the river mouth (Milliman and Farnsworth, 2011). Since 1941, the sediment load in the Colorado River declined by almost 100%,

* Corresponding author.
E-mail address: zjdai@sklec.ecnu.edu.cn (Z. Dai).

http://dx.doi.org/10.1016/j.quaint.2015.01.045
1040-6182/

which caused irreversible damages to its delta (Pitt, 2001). Because of the sediment load reduction, the Niger delta suffered a recession rate of 10 m/y (Ibe, 1996). All of the examples above point to the link between reduction in the river sediment load and the erosion in the estuary, and shoreline recession of the delta at the river mouth.

However, due to the various physiographic characteristics of the river catchment (such as the nature of topography and river bed, spatial scale of the catchment, and degree of human disturbance), the change of suspended sediment load in the upper reaches of a river might not be directly reflected by the load in the lower reaches (Brizga and Finlayson, 1994; Phillips et al., 2004). For example, no dam-related changes in alluvial sedimentation are noticeable in the lower river reaches of southeast Texas, despite large reservoirs control 75–95% of the drainage area, and retention of massive amounts of water behind dams (Phillips, 2003; Phillips et al., 2004). Channel dredging and jetty construction caused the Mersey Estuary lost 0.1% of its volume in the past 150 years (Lane, 2004). Conversely, because of the retaining walls, a large amount of sediment has accumulated in the middle of the Lune Estuary (Spearman et al., 1998). Furthermore, morphological changes of a river mouth and its adjacent coast could also be caused by land reclamation, dredging of navigational channels, relative sea-level rise, and littoral drift (Phillips and Slattery, 2006; Van Landeghem et al., 2009; Evans, 2012). Under multiple influences of the changes in the river runoff and sediment load, changes in the local environment, engineering practices, and changes in the estuarine hydrodynamics, the morphological evolution of an estuarine is complex, and needs a comprehensive approach in the analysis.

The estuary of the Changjiang is located at the end of the longest river in China. The width of the river mouth is almost 100 km wide (Fig. 1). At the river mouth, the mean tidal range is 2.67 m, and the mean flow rate is 1 m/s (Dai et al., 2013a). Three islands, Chongming, Hengsha, and Jiuduan Shoal divide the mouth into 4 channels of North Branch, North Channel, North, and South Passages (Fig. 1b). In the past century, the river mouth has been prograding seaward (Chen et al., 1985). Because of extensive land reclamation, the North Branch has become a tidally dominated estuary (Yun, 2004). Due to the engineering project to maintain a deep navigational channel, the North Passage has become an artificially controlled estuarine channel (Dai et al., 2013a) (Fig. 1). The engineering project started in January 1998 (Fan and Gao, 2009), which consisted of four parts: the river diversion, construction of north and south jetties along the channel, and dredging of the thalweg. The first stage of the project completed in June 2001, which achieved the diversion of the river flow, partial completion of the jetties, and the navigational channel reached 8.5 m depth. The second stage began in May 2002 and lasted until March 2005, in which the jetties with the attached groins along the length of the N. Passage were completed and the navigational channel reached 10 m depth. The last stage commenced in September 2006 and was completed in March 2010, in which the dredging was the main focus and the navigational channel reached 12.5 m depth. Upon the completion of the channel improvement and maintenance project, the deep-water navigation channel was 92.2 km long, 350–400 m wide, having the thalweg depth of 12.5 m (Fan and Gao, 2009; Fan et al., 2012; Dai et al., 2013a) (Fig. 1).

The world's largest dam, the Three Gorges Dam (TGD), located in the upstream of the Changjiang, became operational in 2003. The measured suspended sediment discharge (SSD) at Datong (the upper limit of the tidal river) dropped sharply to 2.06×10^8 and 1.47×10^8 in 2003 and 2004, respectively, in comparison to over 4.2×10^8 t/y before the 1970s (BCRS, 2010, 2011). In 2006, and 2011, the sediment delivered to the sea declined further to be 0.84×10^8, 0.72×10^8 t/y (BCRS, 2010, 2011). Whether the drastic reduction of sediment load is going to trigger erosion or the progradation of the

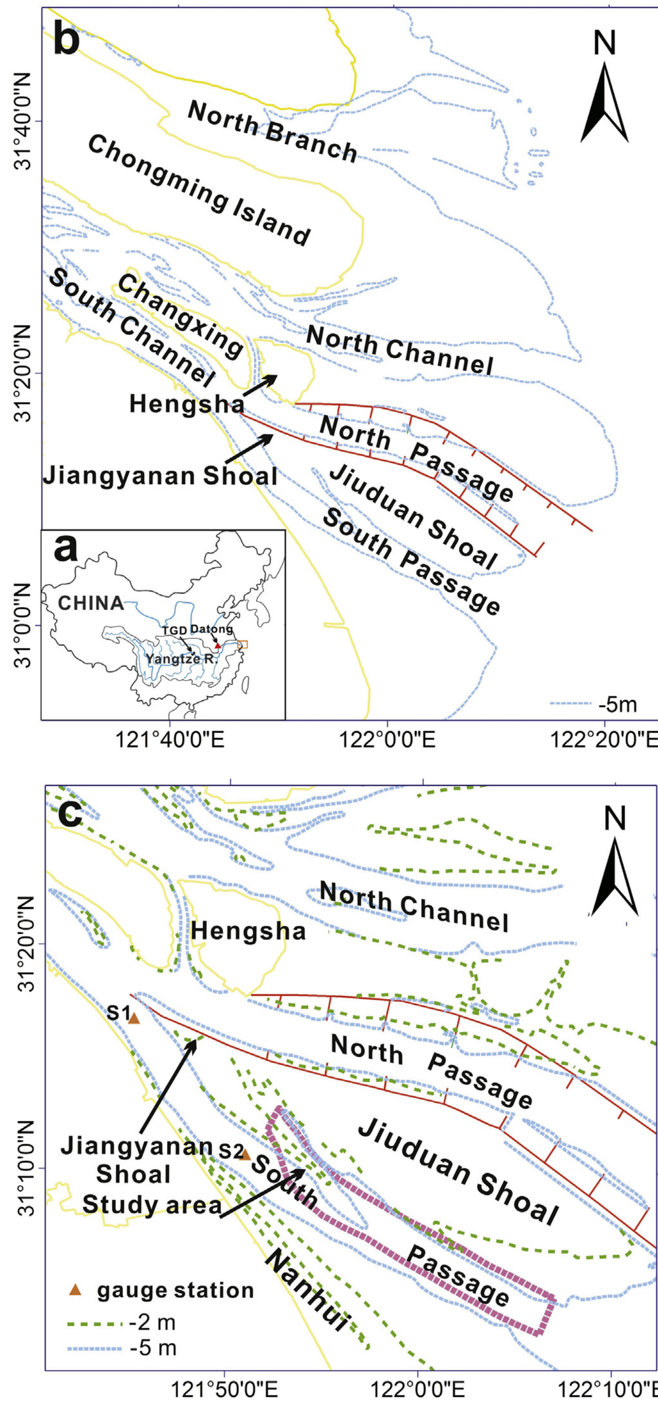

Fig. 1. Maps showing: a. the location of the study area in relation to the China; b. the morphological units at the mouth of the Changjiang based on the 2006 navigational chart; c. the location of the SP and the study area is marked by dashed lines.

Changjiang estuary delta will continue has been an international dispute (Liu et al., 2007; Yang et al., 2007, 2011; Syvitski et al., 2009; Wang et al., 2009; Chen et al., 2010; Dai et al., 2013b; Wang et al., 2013). Based on local cross-sectional changes in the estuary, Yang et al. (2007) found that the reduction of the river sediment load of the Changjiang is the reason for the erosion of estuarine wetlands. However, from the analysis of the morphological changes of the shipping channel along the North Passage, Dai et al. (2013a) found deposition in the peripheral groin fields along the shipping channel and deepening of the shipping channel, which is primarily due to the channel improvement and maintenance engineering. Variability of the river-mouth shoal (seaward migration and size reduction), which is caused by the declining sediment discharge of the Changjiang due to the TGD, and the enhancement of the ebb flow as the result of dredging (Dai et al., 2013a). Furthermore, Jiang et al. (2012) suggest that since 1999 the channel maintenance engineering practices have on one hand limited the seaward progradation, but on the other hand, induced vertical accretion of the Jiuduan Shoal. The combined factors of upstream sediment load reduction and local channel maintenance engineering practices are no doubt making the morphological processes at the mouth of Changjiang more complex.

Since both the North Branch and North Passage have been subject to human alteration (such as local reclamation along the North Branch, channel dredging of the North Passage) (Yun, 2004), it is difficult to distinguish natural from the anthropogenic causes of morphological development. Although the North Channel has the least human interference, it is not the major conduit for the export of riverine sediment, and it has been the least studied. However, the South Passage (SP), being the major conduit for water and sediment of the Changjiang (Milliman et al., 1985), has also been affected by direct human activities to a limited extent. Since 1987, this channel has been monitored for navigational purposes with uninterrupted yearly nautical topographic records. Thereafter, the objective of this paper is to diagnose the decadal morphological changes of this channel to determine the whether the decline of distal river sediment source or the proximal local influences would affect the developtment of the SP. The outcome will be valuable to assess the potential response of part or the whole of the Changjiang Estuary to the upstream reduction of sediment supply, and the impact of the natural and man-made factors near and far. It could be applied to river estuaries with similar distributary mouths worldwide that are also under similar natural and anthropogenic influences.

2. Material and methods

Digitized bathymetry-derived DEM has become a useful tool to study morphological changes of estuaries (Thomas et al., 2002; Van der Wal et al., 2002; Lane, 2004; Blott et al., 2006; Jaffe et al., 2007). This study collected surveyed bathymetric data of the SP since 1987. The 1987–2000 data came from published nautical charts by the Maritime Survey Bureau of Shanghai, Ministry of Communications of China. The data for 2001–2012 came from the nautical charts published by the Changjiang Estuary Waterway Administration Bureau (CJWAB), Ministry of Transportation of China (Table 1).

Table 1
Observed water depth data in the South Passage, Changjiang.

Surveyed date	Map title	Scale	Data sources
1987, 1988, 1989, 1990, 1990, 1991, 1992, 1993, 1994, 1995, 1996, 1997, 1998, 1999, 2000	Nancao Fairway	1:50000	MSBSMCR[a]
2001, 2002, 2003, 2004, 2005	Beicao and Nancao Fairway, Changjiang Estuary	1:25000	CJWAB[b]
2006, 2007, 2008, 2009, 2010, 2011, 2012	Beicao and Nancao Fairway, Changjiang Estuary	1:10000	CJWAB

[a] MSBSMCR: Maritime Survey Bureau of Shanghai, Ministry of Communications of China.
[b] CJWAB: Changjiang Estuary Waterway Administration Bureau (CJWAB), Ministry of Transportation of China.

All the bathymetric surveys were conducted in August or September each year based on the theoretical low-water datum. Dual-frequency echo sounders and GPS positioning were used. The vertical error was limited to be within 0.1 m. Survey density consisted of 8–20 bathymetric data points per km^2. Maps of the Changjiang Estuary and SP with the same precision have been applied to studies on estuarine erosion and deposition (Yang et al., 2011), evolution of the river trough (Jiang et al., 2012; Wang et al., 2013; Dai et al., 2013a), and the morphological changes of the estuary and submerged delta (Dai et al., 2014). Tthe morphological changes in the current study exceed 0.1 m. Accordingly, the surveyed the digital data of the SP is reliable to use for the study of the morphological changes of the SP.

All charts were georeferenced using nine fixed benchmarks, of which the National Grid coordinates were known. The depth values were converted to elevation relative to Beijing-1954 Datum. After obtaining the charts, we digitized them by using ArcGIS 9.3 as the platform for input, output, and comparison. The Kriging scheme was used to interpret the digitized data into grid having resolution of 250 × 250 m.

In the meantime, we collected the river flow data in the study area (source: CJWAB). The tidal flow was measured at S1 and S2 in the SP in the flood season of August in 2002, 2005, 2007, and 2010, respectively (Table 2). The measurements at the two locations were synchronized and took place during spring tide and lasted over 25 h.

Table 2
Hydrological gauging stations of the South Passage

Stations	Position	Surveyed periods
NC1	121.76° E, 31.27° N	8.2002, 8.2005, 8.2007, 8.2010
NC2	121.85° E, 31.19° N	8.2002, 8.2005, 8.2007, 8.2010

This study also collected the river runoff and suspended sediment load at the Datong station located at the landward limit of the tidal river (Fig. 1, Hydrological Committee of Changjiang, www.cjw.com.cn) (BCRS, 2010, 2011).

At each hydrographic station, the coefficient of flow dominance (defined as tidal flow rate during the ebb divided by the sum of tidal flow rates of the ebb and flood) was calculated (Simmons, 1955) as follows:

$$A = \frac{Q_e}{Q_e + Q_f} \times 100\% \tag{1}$$

in which A is coefficient of dominance flow, Q_e is cross-sectionally averaged ebb flow rate, Q_f is cross-sectionally averaged flood flow rate. When $A > 50\%$, the flow is ebb-dominant. Conversely, it is flood dominant.

To quantify morphological changes, the −5-m isobath was extracted through the ArcGIS platform. From ArcGIS the maximum and mean water depths of each chart were obtained. To quantify erosion/deposition, the volume changes were calculated at 3–4 year increments between 1987 and 2012, which included 26 yearly charts. The spatial and temporal correlations (standardized covariance) of the water depths in the 26-year period were then analyzed by using the multivariate analysis technique EOF (Empirical Orthogonal/Eigen Function) analysis.

EOF is a classical statistical technique, which was used to separate orthogonal modes contained in the data sets (Liu et al., 2000). The advantage of using EOF analysis is that a set of inter-correlated variables can be decomposed into a set of statistically independent modes, which bear physical meanings. Thus, the EOF technique has been widely applied to problems in meteorology, oceanography, geology, and sedimentology (Liu et al., 2000; Emery and Thomson, 2001; Liu and Lin, 2004; Lane, 2004; Dai et al., 2013a). Here, all the standardized bathymetric variance sets can be deviated to form a single matrix X

$$X = (X1 \ldots Xn)$$

where each Xn represents a single grouped observation of the m variables and X is an $m \times n$ data matrix. m is the number of spatial points, and n is the observed time points.

Mathematically, the EOFs are the eigenfunctions of the covariance matrix S, which is given by $S = XX'$. Based on singular value decomposition of the matrix S, the eigenvalues $\lambda = (\lambda_1, \lambda_2, \ldots, \lambda_m)$ of S and spatial patterns (V) can be obtained. Thereafter, the time series describing the loadings (T) can be obtained by $T = V'X$ (Wallace and Dickinson, 1972).

Subsequently, eigenvalues $\lambda = (\lambda_1, \lambda_2, \ldots, \lambda_m)$ can be ranked according to the amount of data (covariance) they explained, i.e. the variance contribution of each eigenvalue R_K, and the cumulative contribution for the eigenvalues G can be considered as:

$$R_k = \frac{\lambda_k}{\sum_{i=1}^{m} \lambda_i} \quad [k = 1, 2, \ldots p(p < m)]$$

$$G = \frac{\sum_{i=1}^{p} \lambda_i}{\sum_{i=1}^{m} \lambda_i} \quad (p < m)$$

Generally, the better correlated the data are, the more covariance can be accounted for by the first few eigenmodes (Liu et al., 2000; Emery and Thomson, 2001). The remnant eigenfunctions are neglected due to the effect of noise contained in this set (Wallace and Dickinson, 1972).

3. Results

3.1. Bathymetric changes along the SP

Jiangyanan Shoal is located at the upstream opening of the SP. Prior to 1997, Jiangyanan Shoal and Jiuduan Shoal were disconnected, as the downstream part of the South Channel (Fig. 2a). Currently, Jiuduan Shoal is located on the north side of the SP, and Nanhui Shoal is on the south side of the SP (Figs. 1c and 2b). Based on the changes of the location of the −5-m isobath (Figs. 1c and 3), the morphological changes at the SP can be characterized by 2 stages. In the first stage of 1987–1997 there was a single channel at the SP, which is clearly shown in the nautical chart of 1990 (Fig. 2a). In the early period of this stage the −5-m isobaths of Jiangyanan Shoal and Jiuduan Shoal were not connected. There was a short channel about 1 km wide separating the two sand bodies (Fig. 3a), allowing exchange between the North and South Passages. Along the south side of the SP there was a ‘spur’ on the −5 m isobath pointing to the spit of the Jiangyanan Shoal (Fig. 3a). In the following years of 1990–1994, the −5-m isobaths of Jiangyanan and Jiuduan Shoals connected. The north side of the short-cut-channel was filled in. In the meantime, the spit at the southern end of the Jiangyana Shoal migrated northward by 1260 m (Fig. 3b) but the thalweg of the SP was located toward the north side of the channel along Jiuduan Shoal. In 1994–1997, the short-cut-channel was completed closed as shown by the −5-m isobath. The spit of Jiangyanan Shoal was eroded by 1060 m (Fig. 3c). The Jiangyanan Shoal and Jiuduan Shoal were merged so that the bank of SP extended to include the Jiangyanan Shoal. Thereafter, between 1987 and 1997, with closure of the short channel, the SP had a single stable channel. As a result, the SP had a relatively straight thalweg. The short-cut-channel became a wide flood cove.

In the second stage of morphological changes in 1997–2012, the spit of the Jiangyanan Shoal elongated downstream, making the opening of the SP into a dual channel system (Fig. 3d and e). In the period of 1997–2000, the erosional pattern of the spit turned to accretionary and the spit extended downstream by 6430 m. In the same time, the −5-m isobath of the southern bank of the SP extended northward, to form a narrow gap of 800 m between the spit of the Jiangyanan Shoal and the southern bank of the SP (Fig. 3d). The flood cove between the two shoals narrowed and its northern end moved downstream by 1670 m in response to the elongation of the spit (Fig. 3d). In 2000–2003, the spit of Jiangyanan Shoal continued to accrete into the relative stable channel of SP by 2380 m. However, the entire spit shifted northward by 1300 m together with the flood cove on its north side (Fig. 3e).

As the spit of the Jiangyanan Shoal grew in the southwestern direction, the SP became a shoal–trough complex, which is clearly reflected in the 2006 nautical chart (Fig. 2b). The spit increments in the periods of 2003–06, 06–09, and 09–12 were 1200, 4100, and 3500 m, respectively. The flood tidal cove on the north side of the spit became narrower (near 800 m in 2006 and less than 500 m in 2012). Comparing to 2009, the position of the flood tidal cove moved NW by 6800 m (Fig. 3f–h). Cross-sectional wide, due to the

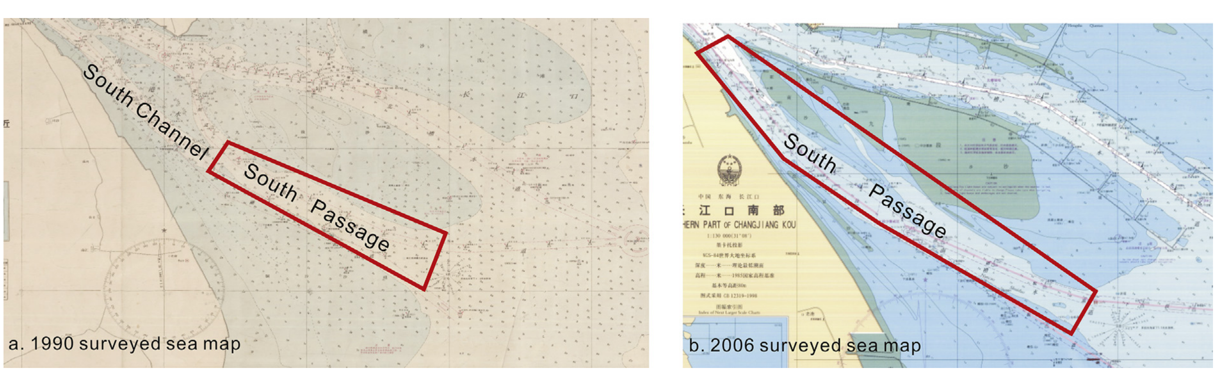

Fig. 2. Nautical charts of a. 1990, and b. 2006.

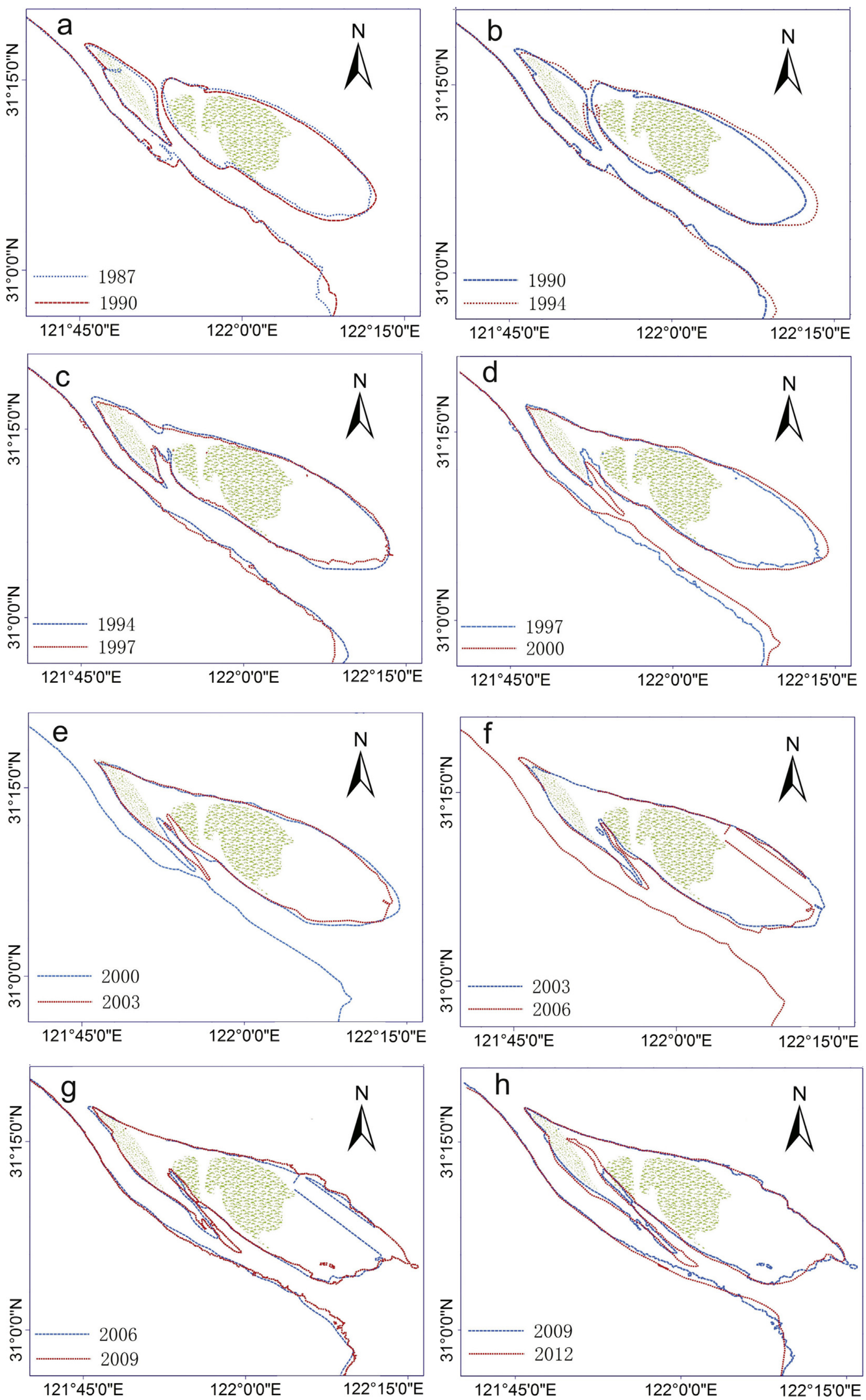

Fig. 3. Geomorphological changes of the SP and the two shoals as expressed by the −5-m isobath in 3-y increments.

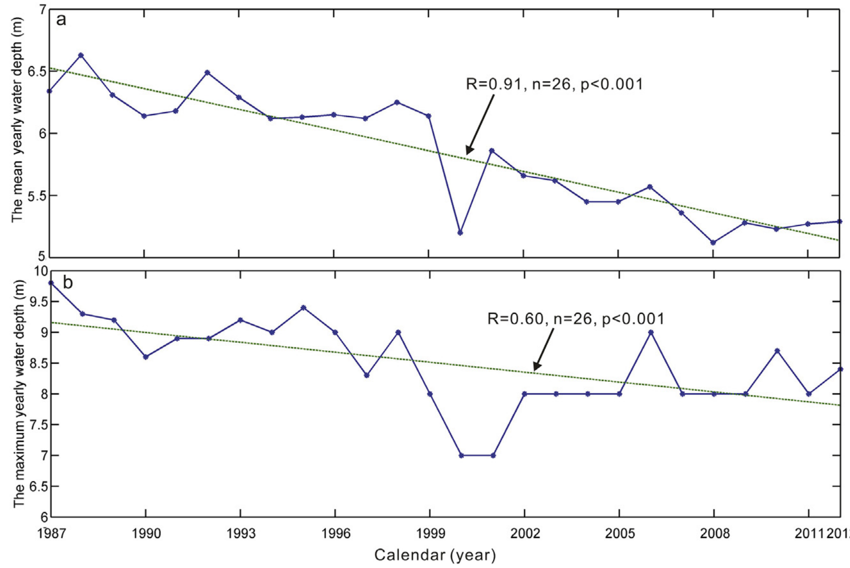

Fig. 4. Water depth changes of the SP in 1987–2012: a. yearly mean depths; b. yearly maximum depths.

downstream accretion of the spit in the upper part of SP, the lower part of the SP deepened and the thalweg remained closer to the Jiuduan Shoal. Thus, the present-day SP formed a complex morphology.

3.2. The bathymetry and associated volume change at the SP

The yearly average water depth of the study area in the 30-year period between 1987 and 2012 fluctuated between 5.1 and 6.7 m, by over 1 m, but also showed a decreasing trend (Fig. 4a). A sudden drop over 1 m occurred in 1999. During the same period, the maximum water depths also showed a decreasing trend (Fig. 4b), which had a sudden decrease from 9 m in 1998 to 7 m in 2000, also reflected in the drop of the yearly mean depth (Fig. 4a).

The volume capacity of SP has been gradually decreasing from 0.69×10^9 m^3 at 1987 to 0.59×10^9 m^3 at 1994, a reduction by 14% (Fig. 5), implying infilling of the SP. In 1994–1996, the capacity increased by 0.04×10^9 m^3. After 1998, the capacity continued to decrease. In 2001–2006, the capacity increased slightly. In 2006–2008, the capacity dropped drastically by 0.06×10^9 m^3, and then gradually gained back slightly. Overall, between 1987 and 2012, the volume capacity of SP lost about 13% (Fig. 5). Comparing to the 0.1% volume decrease of the Mersey Estuary in the past 150 yr (Lane, 2004), the decrease at SP is considerable.

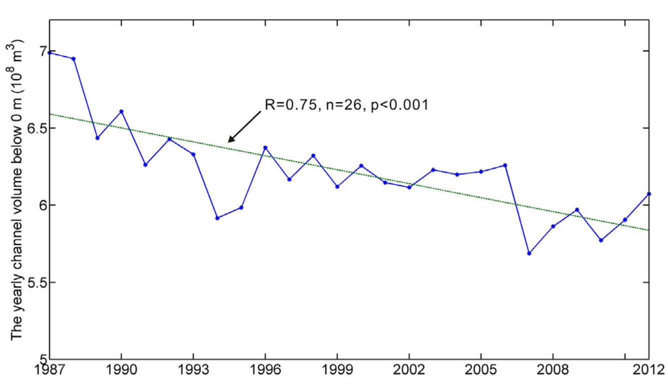

Fig. 5. The volume capacity change below the 0-m isobath of the SP in 1987–2012.

3.3. Deposition/erosion of the SP

Visual comparisons of the depth changes in 3–4 y increments (Fig. 6a–h, 7) indicate that the stages of erosion/deposition patterns of the SP were identical to the 2 stages described earlier. In the first stage (1987–1997) the SP was more or less in erosion/deposition equilibrium, having slight tendency of deposition. Because of the joining of the spit of Jiangyanan Shoal and the Jiuduan Shoal, the upstream part of the SP turned from erosional (by 1 m) to depositional (by 1 m) (Fig. 6b and c). The overall deposition was about 0.2 m.

In the second stage (1997–2012), SP was firstly in the state of adjustments during 1997–2003 (Figs. 5d, 6e and 7). This is strongly reflected by the deposition around the upstream opening of the SP. Compared to the previous period of 1994–1997 (Fig. 6c), in the period of 1997–2000 the entire SP experienced slight net erosion. The erosional rate was over 5 cm/y (Fig. 7). In 2000–2003, the total accumulation around the upstream opening of the SP was over 4 m. In contrast, around the seaward opening near Jiuduan Shoal, the total accumulation was over 3 m in 1994–1997. In 1997–2000, the erosional rate was over 6 cm/y (Fig. 7). But in 2000–2003, a slight accumulation rate of about 10 cm/y occurred (Fig. 7). From 1997 to 2003, the net change at SP was from an erosion rate of 5 cm/y to an accumulation rate of about 10 cm/y (Fig. 7).

In the subsequent years during 2003–2012, the SP was in a state of strong deposition that had a net accumulation rate over 10 cm/y (Fig. 7). Within this trend, localized strong erosion and deposition also occurred (Fig. 6f–h). These areas included the continued accumulation at the upstream opening of the SP by 1–2 m. The southern end of the SP on the other hand, was in the state of erosion by about 1–2 m. Deposition also occurred in the center section of the SP, on average about 1 m. Since 2003–2009, the deposition area in the center-channel gradually moved upstream (Fig. 6f and g). In 2009–2012, the entire SP was in a general state of accumulation (average rate of 10 cm/y) except for a narrow zone of erosion over 1 m along the center section of Jiuduan Shoal (Figs. 6h and 7). Thereafter, between 1997 and 2003, the SP went through another period of erosion/deposition adjustment during which the opening of the SP developed a two-channel morphology (Fig. 7), which stabilized and showed infilling during 2003–2012 (Fig. 7). In this entire period (1997–2012) the changes included eastward spit

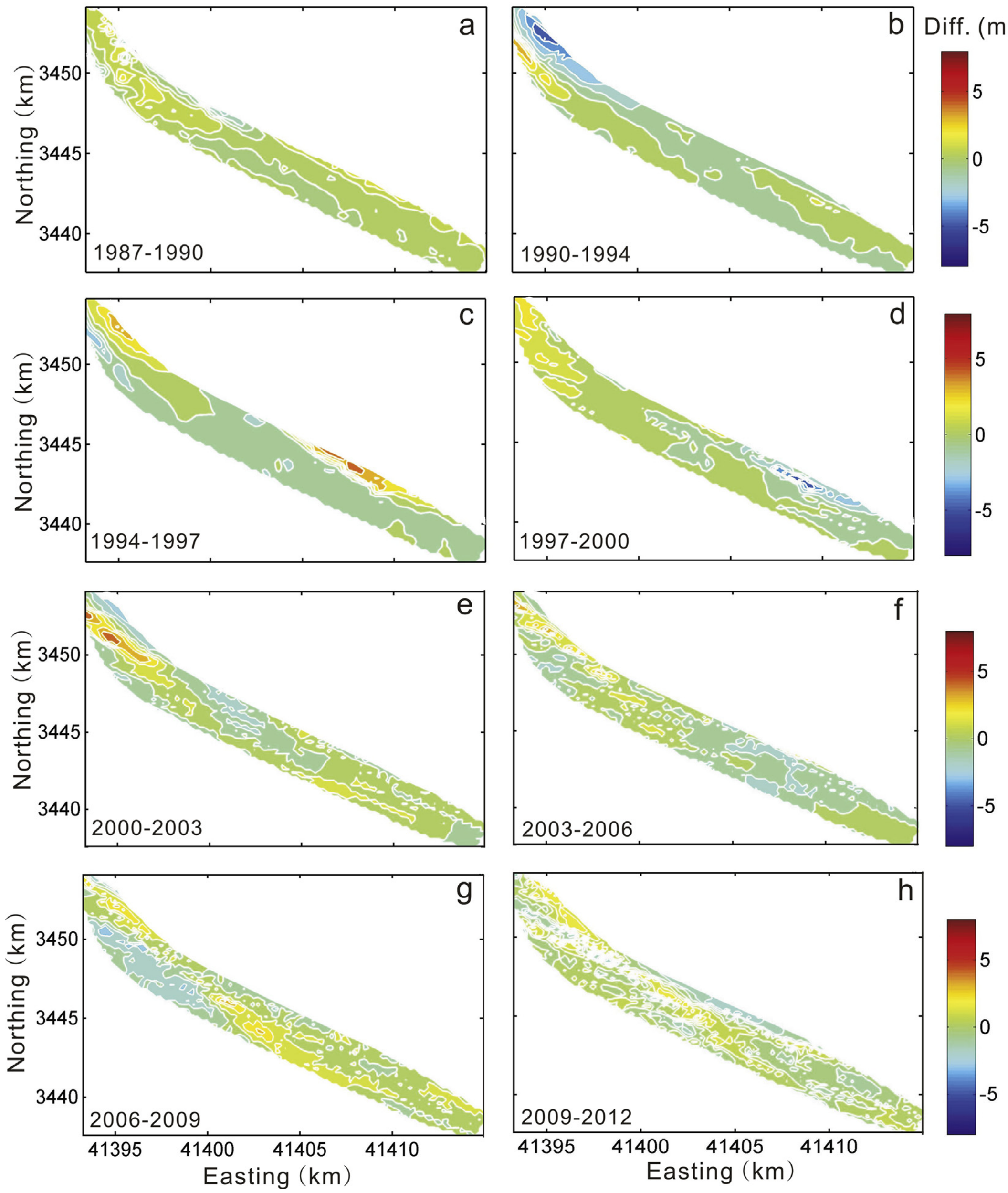

Fig. 6. Erosional/depositional patterns of the SP (negative means erosion, positive means deposition) in different time periods.

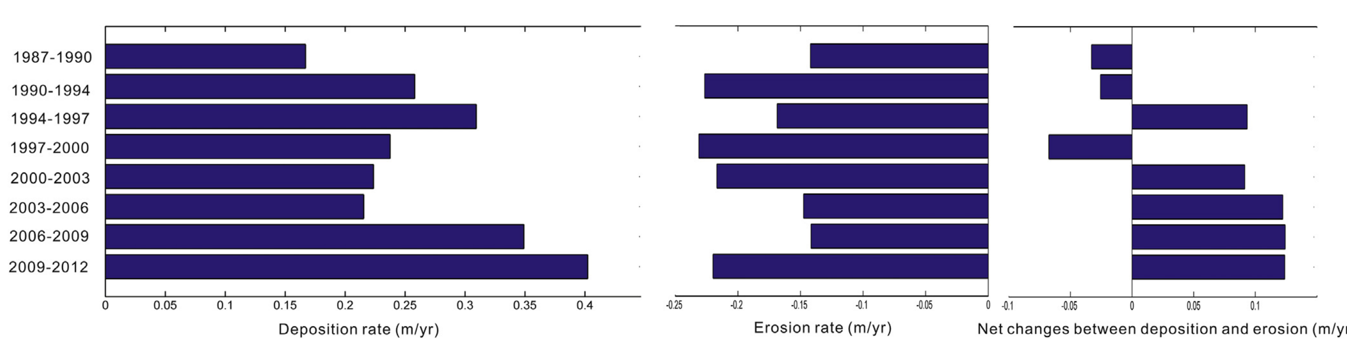

Fig. 7. The net erosion/deposition values of the SP derived from Fig. 6.

formation and westward shoal incision of the short channel, eastward spit formation and westward shoal incision of the cross-channel.

3.4. EOF analysis of the bathymetric changes

The results of EOF analysis on the water depth data from 1987 to 2012 show that the first two eigenmodes can explain over 75% of the standardized covariance of the data (Fig. 8). As all higher modes explain less than 10% of the data, only the first two modes are presented and discussed.

The first eigenmode explains 59% of the water depth co-variability, which is the most important form of morphological changes. The contour plot of the eigenvectors of this mode shows the spatial co-variability in the SP including the accretion at the center of the northern opening of the channel (the area of highest positive values) due to the sediment load input from upstream and along the south side of the Jiuduan Shoal (Fig. 8a). Also, along the northern edge of the SP bordering the Jiuduansha there is an elongate area having values of 0–0.05. These are the areas of aggradation whose temporal pattern shows increasing trend as indicated by the eigenweighting curve of this mode (Fig. 8b). This mode also shows the formation of the thalweg in the center of the channel. The temporal pattern of this mode is expressed by the eigenweighting curve of this mode (Fig. 8b), which shows an increasing secular trend, which resembles the inverse trends of the decreasing mean water depth, maximum depths (Fig. 4a and b), and the decreasing volume capacity (Fig. 5). Therefore, this mode describes the increasing spatial gradients in sediment transport into the SP whose most significant effect is shown by the major deposition in the upstream opening of SP depicted by the eigenvectors (Fig. 8a).

The second mode explains the 18% of the water depth co-variability. The eigenvectors of this mode indicate that the morphological changes related to the growth, decay and movements of the spit of the Jiangyanan Shoal, which is the second most important factor contributing to the water depth changes in the SP (Fig. 8c). The 'W' shaped temporal pattern suggests a somewhat recurring pattern, if not cyclical. From 1987 to 1995, the descending trend in the eigenweighting curve reflects the retreat of the spit of the Jiangyanan Shoal (Figs. 8d and 3). On the other hand, the rapid downstream elongation of the spit caused the ascending trend between 1995 and 1998 (Figs. 8d and 3). Between 1999 and 2002 the spit retracted and became shorter. In the meantime, it migrated towards the Jiuduan Shoal, making the tidal cove narrower (Figs. 8d and 3). Beginning in 2003, the spit began to lengthen again, accompanied by the erosion and the head-ward retrogression of the cove, making it resemble a narrow and long channel (Fig. 3f). This development is reflected by the ascending part of the eigen-weighting curve after 2003 (Fig. 8d).

4. Discussion

4.1. The changing sediment load of Changjiang

The average water discharge of Changjiang exceeds 900×10^9 m^3/y. The runoff of the Changjiang did not show noticeable change in the period between 1954 and 2011 (Fig. 9a). The mean sediment load of the Changjiang is 420×10^6 m^3. In the period of 1954–2011 there was a decreasing trend, which was more pronounced in the period of 1987–2011 (Fig. 9b). In the case of the NP (Fig. 1a), the accumulation is on the order of hundreds of million tons despite the sediment load reduction (Jiang et al., 2012; Dai et al., 2013a). This is largely attributed to the engineering works (Dai et al., 2013a). The regions shallower than the −5-m isobath on the submerged delta of the Changjiang was still in the state of accretion (Yang et al., 2011). Controversy continues regarding whether or not the shores around the mouth of Changjang will start to erode (Chen et al., 2010; Yang et al., 2011; Dai et al., 2012, 2013a; Wang et al., 2013).

Sediment supplied by the Changjiang determines the seaward progradation of its river mouth (Chen et al., 1985). Since the 12th century, the shoals on the south bank of the Changjiang have prograded seaward at the pace of 1 km per 40 y. In the last half century, the rate accelerated to 1 km per 23 y (Chen et al., 1985). Since the SP is the major seaward conduit of the riverine sediment (Milliman et al., 1985), it should show responses to the load reduction. The relations among the maximum water depth, mean depth, and the whole capacity below 0 m isobath of the SP and the sediment load of Changjiang into the estuary in the period

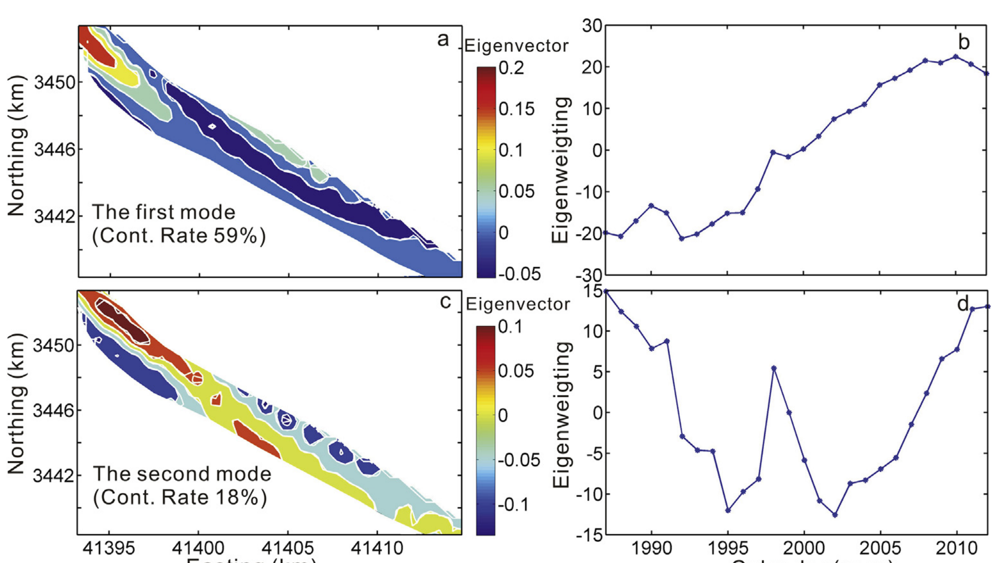

Fig. 8. The EOF analysis result of the time-space related water-depth changes Showing: a. the plot of the 1st mode eigenvectors; b. the 1st mode eigenweighting curve; c. the plot of the 2nd mode eigenvectors; and d. the 2nd mode eigenweighting curve.

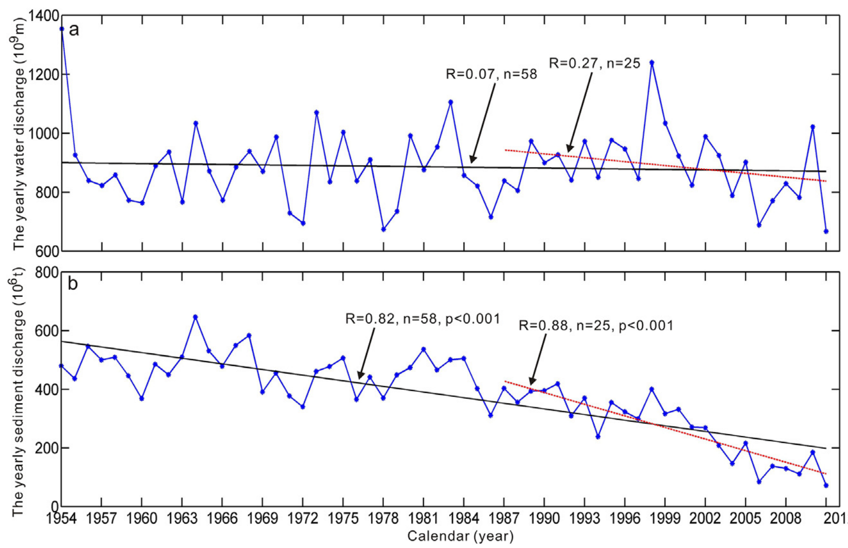

Fig. 9. Yearly records of discharge (a), and suspended sediment load (b) at the Datong st. The black lines are the linear regression results for the period of 1954–2011 and the red lines are the linear regression results for the period of 1987–2011, respectively. (For interpretation of the references to colour in this figure legend, the reader is referred to the web version of this article.)

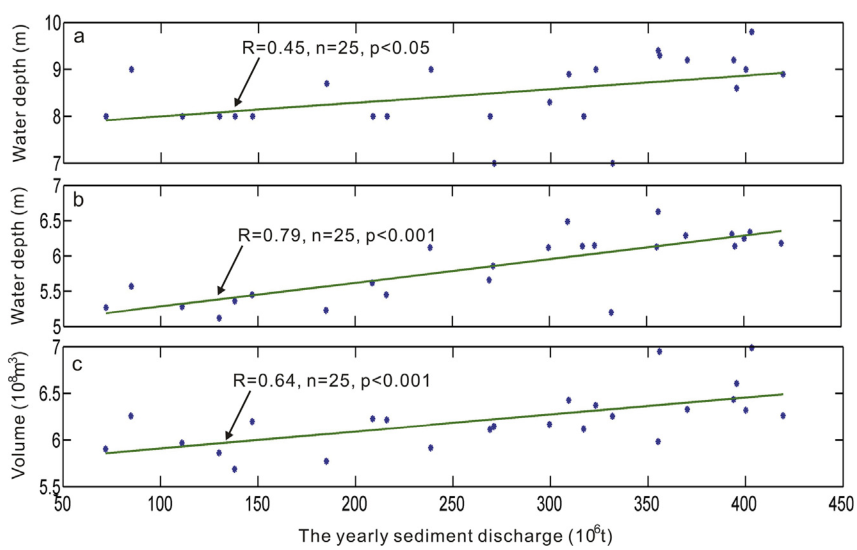

Fig. 10. Yearly mean sediment load at Datong st. verses (a) yearly max. water depth; (b) yearly mean water depth; and (c) volume capacity below the 0-m isobath of the SP.

1987–2011 show statistically significant ($p < 0.001$, except for the maximum water depth) positive correlations (Fig. 10a–c). These patterns indicate that the decrease in mean and maximum water depths and the volume capacity of the SP are associated with the reduction of the sediment supply, which is counter-intuitive. The value of mean grain-size of the Changjiang sediment was 0.0017 mm (1976–2000) and that of the medium diameter in 2012 was of 0.011 mm. The fining trend corresponds with the deposition trend in the SP, attesting to the deposition in the SP. On the other hand, reduction of sediment supply should have induced erosion, which in turn would have caused deepening of the SP and an increase of the volume capacity. However, the above relations point to factors other than these direct distal effects of the reduction of sediment supply upstream of the Changjiang Estuary. This is consistent with the recent discovery that the despite the reduction of the distal sediment source, the submerged delta of the Changjiang still showed aggradation (Dai et al., 2014) due to proximal and local factors.

4.2. Local influences

Engineering works in the NP have affected the Jiangyanan and Jiuduan Shoals. The construction of the south jetty and dike system in the NP stabilized the northern rim of these two shoals. From the second stage to the end of the third stage of the navigation channel improvement and maintenance project the flow dominance coefficient measured at the two stations in the SP first showed decreasing and then increasing trends (Fig. 11). The minimum ebb dominance was 60%, which reached 70% during the flood season of 2010. These trends indicated the engineering practices of the project strengthened the ebbing flow, which enhanced the channel's ability to transport sediment seaward (Fig. 11). Furthermore, the engineering structures blocked the sediment exchanges between the NP and SP (Yang et al., 1998; Li et al., 2006). This is reflected by the disappearing of the short-cut-channel before the early 1990s (Fig. 3a–c). In 1997–2006, during slack transition from flood to ebb, the suspended sediment in the NP was still able to

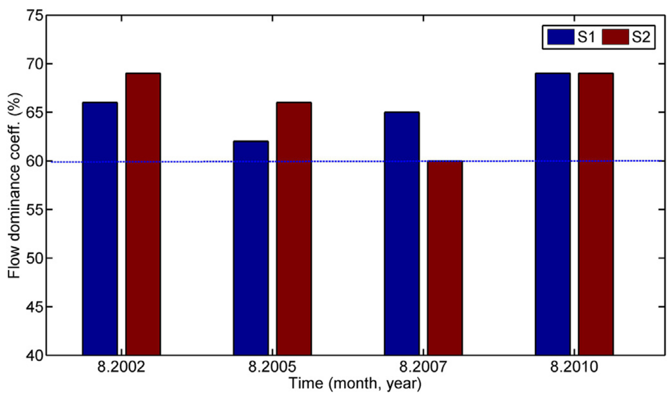

Fig. 11. The measured flow dominance coefficients at two hydrographic stations at different times.

move over the submerged dike and enter the SP (Liu et al., 2010). Since the peripheral groin field of the NP trapped sediment, this could be a local source for SP. The depositional pattern along the Jiuduan Shoal illustrated by the 1st mode eigenvectors (Fig. 8a) could be the effect of this source. However, this sediment input from NP did not fully fill in the tidal cove, which remained stable (Fig. 3d–g). Rather, sediment could probably bypass the cove and enter the main channel of SP. In 2012, the cove almost cut Jiangyanan Shoal in the form of head-ward erosion, which was potentially caused by the cut-off of spill-over sediment from the NP.

Moreover, the SP has not been significantly affected by land reclamation, which was carried out on the tidal flat of Nahui on the south bank of the SP in 1994–2003 (Figs. 1b and 12) (Li et al., 2007). At present, the reclaimed area above the −2 m isobath exceeds 15, 000 hm^2 (Li et al., 2010). Although the geomorphology of SP in 1987–2012 has shown appreciable changes (Fig. 3) in the river channel, but the positions of the −5-m isobath on both sides of the SP remained unchanged and relatively stable. This suggests that reclamation-engineering projects at the seaward end of the SP had little influence on the SP morphology, although there may have been an impact on shallower areas.

4.3. Spit morphodynamics of the Jiangyanan Shoal

The EOF analysis points out that the most important mode of morphological change is characterized by the deposition around

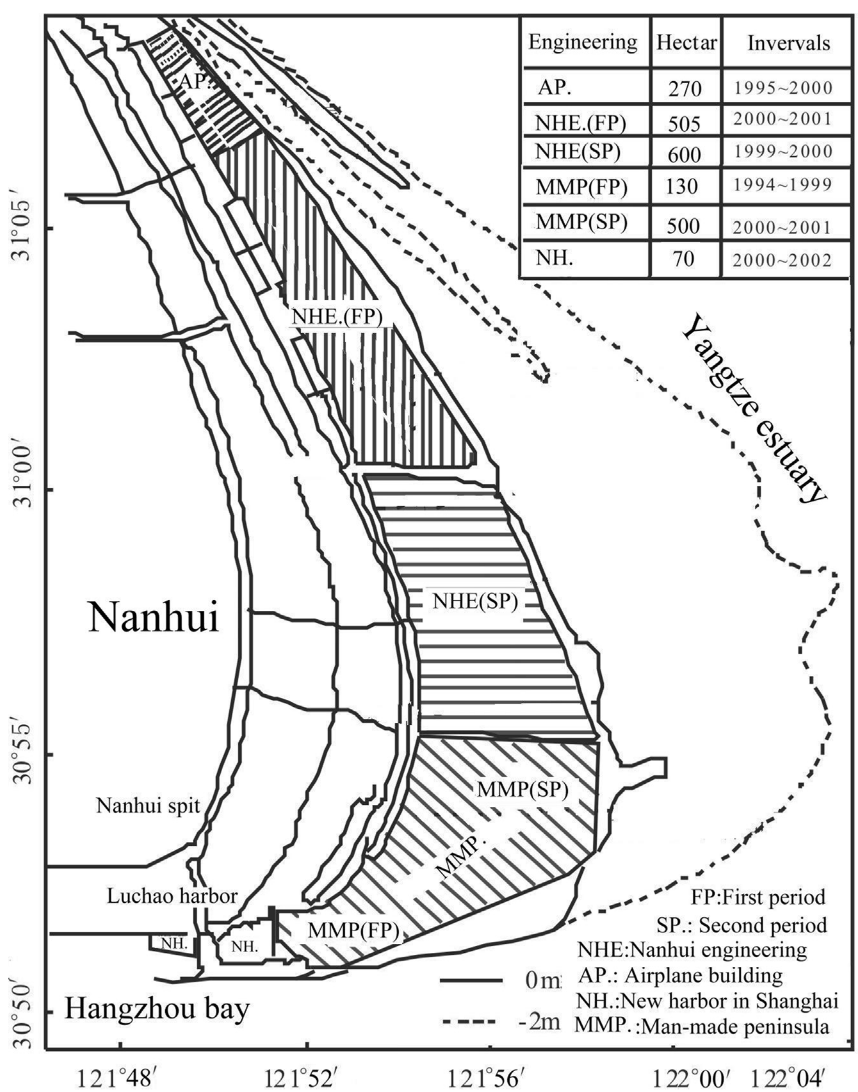

Fig. 12. Schematic plot of the land reclamation of the Nanhui Shoal (Modified from Li et al., 2007).

the northern opening of the SP. To further illustrate a possible proximal sediment source, the development and evolution of the Jiangyanan Shoal is expressed by the 0-m isobath at discrete time points from 1994 to 2009 (Fig. 13).

In 1994, only a few small-scattered sand bodies were present at the general location of the present Jiangyanan Shoal following its orientation (Fig. 13a). In 1997, the size of the sand bodies increased and they continued to develop along the orientation of the Jiangyana Shoal (Fig. 13b). In 1999, the small bodies merged into one large body forming the Jiangyanan Shoal (Fig. 13c). In the meantime, the southern limit of the shoal moved 990 m downstream compared to the 1997 location. In 2002, Jiangyanan Shoal moved downstream by another 3000 m, whose southern tip was separated from the main body to form a small sand body (Fig. 13d). In 2006 the Jiangyanan Shoal moved farther downstream by 1990 m as one body (Fig. 13e). In 2009 the Jiangyanan Shoal moved 1700 m and the elongated spit was well formed (Figs. 3g and 13f). These historic changes suggest the development and downstream movements of the Jiangyanan Shoal also contributed to the infilling of the SP.

The downstream movement was probably associated with the lateral expansion of the Jiangyanan Shoal into the subaerial SP channel, which also can be reflected by the 0-m isobaths (Fig. 13). The downstream movement of the shoal was facilitated by the bed material along the SP. In the Changjiang Estuary, shoal movements are a major form of bedload sediment transport that amounts to 350×10^6 t/y (Li, 1993; Li et al., 2010). This amount is equivalent to the amount of sediment delivered by the Changjiang to the sea, which on a large degree, results in the shoaling of estuary channels (Li, 1993; Li et al., 2010). Generally these shoals comprise of fine sand having the medium diameter of 0.16 mm (Zhou, 1983). Under strong ebbing flow (average velocity: 1–1.5 m/s) the sediment transport in shallow part of the Changjiang Estuary is in the form of sand wave movement, whose migration rate could reach 300–2000 m/y in the flood season (Zhou, 1983; Li, 1993; Gong et al., 2003). Li (1993) described the mechanism of the sand wave migration. This implies that the sediment on the Jiangyanan Shoal could move into SP via sand waves. Thereafter, the temporary trend of the 1st eigenmode thus, could also reflect the enlargement of the Jiangyanan Shoal, which is reflected by the deposition next to the shoal.

The second most important pattern of morphological changes was caused by the slow accretion, recession, and lateral migration of the spit of the Jiangyanan Shoal (Fig. 3a–h). In 1997–2000, the spit extended into the SP channel by 6430 m. The extension caused the single-channel thalweg to become a double-trough channel (Fig. 3d–f). Moreover, the spit also displaced the thalweg and made it shift laterally (Fig. 3). A critical time point in the spit-morphodynamics is 1998 when historically the second most severe flooding in Changjiang occurred (Fig. 9). The river discharge exceeded 120×10^9 m^3. The strong river flow and large amount of sediment load probably triggered the spit of the Jiangyanan Shoal to extend downstream, causing the mean water depth to decrease noticeably between 1998 and 2000 (Fig. 4). Once this spit was in place, in the ensuing years, the spit-building process continued with fluctuations.

At present, the dikes along the south side of the navigation channel stabilized the northern rim of the Jiangyanan Shoal. Jiuduan Shoal is in the state of equilibrium (Jiang et al., 2012). As the reduction in the sediment load from the upstream continues, and the strength of the river flow remains unchanged (Fig. 11), the spit in the SP might not continue to extend downstream. The SP might revert to a single trough channel and the seaward extension of the Jiangyanan Shoal might slow down or stop, and the Jiuduan Shoal might undergo erosion.

5. Conclusions

Having a branching estuary, the Changjiang has one of the most complex river mouths in the world. In the face of declining sediment supply and extensive engineering practices, different channels of this branching estuary have displayed differential morphological processes as followed as:

1. Between 1987 and 2012, the average, maximum, and the volume capacity below the 0-m isobath were all in a decreasing trend. The volume capacity in the last 30 years has decreased by

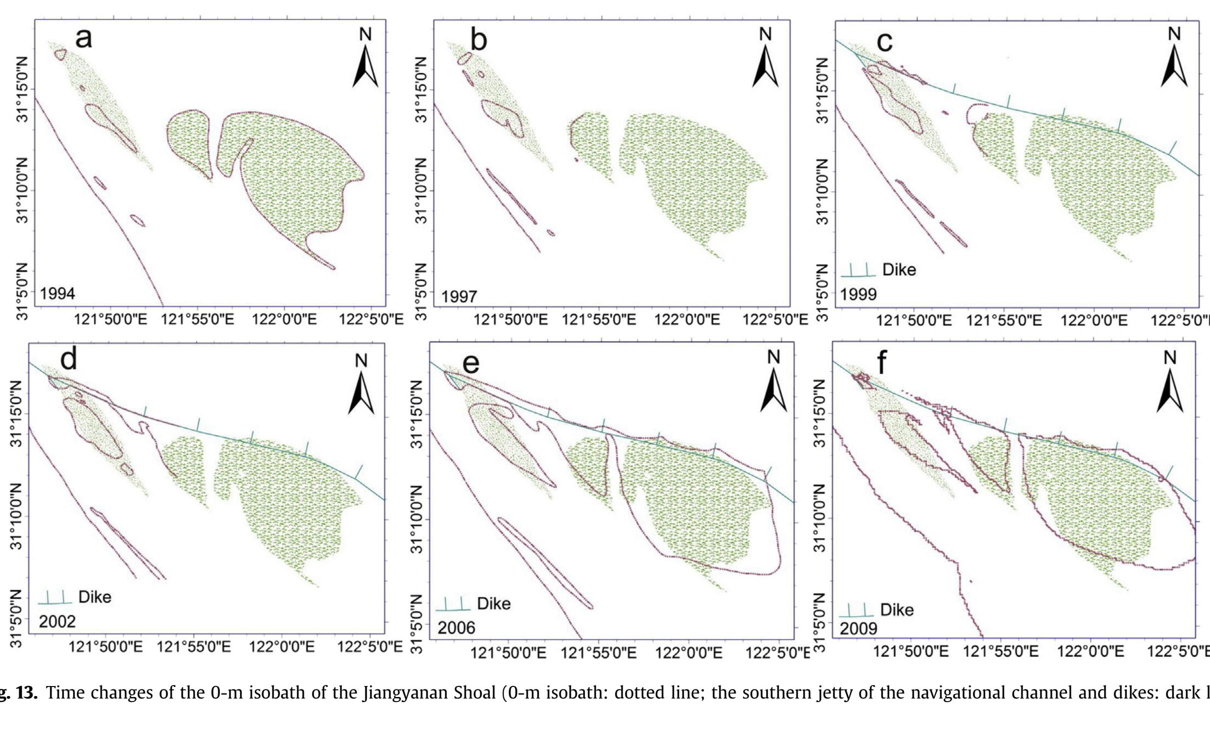

Fig. 13. Time changes of the 0-m isobath of the Jiangyanan Shoal (0-m isobath: dotted line; the southern jetty of the navigational channel and dikes: dark line).

13%. The erosion/deposition patterns varied in time. In 1987–1997 the SP was in a state of equilibrium. The net depth change was 0.2 m. In 1997–2003, the SP was in a state of transition, which was followed by a state of infilling by the amount of 10 cm/y between 2003 and 2012. The infilling is the most important mode of morphological changes indicated by the EOF analysis result, which is mostly attributed to the deposition in the northern opening of the SP.

2. There were two stages in the morphological processes at the SP. Between 1987 and 1997 the SP had a single channel with closure of the cross-channel. Between 1997 and 2012, the SP firstly transitioned from a single channel to a two-channel configuration from 1997 to 2003. From 2003 to 2012, the SP remained a two-channel branch. In this period SP showed eastward spit formation and elongation and westward shoal incision of the cross-channel. These two stages were controlled by the lengthening, retreat, and lateral migration of the spit of the Jiangyanan Shoal, which is the second most important mode of morphological changes indicated by the EOF analysis results.
3. The secular trend in the sediment load decrease cannot explain the opposing trends of water depth and volume capacity decrease at the SP. The morphological changes in the SP were mainly induced by the development, growth, and migration of the Jiangyanan Shoal into the SP and the morphodynamics of the spit of the Jiangyanan Shoal. Furthermore, the engineering project north of the SP stabilized the river flow partition and constricted the ebbing flow to be stronger as shown by the high coefficient of ebb-flow dominance. This might help to transport sediment into SP from the upstream.

Acknowledgements

This study was supported by the National Science Foundation of China (41476076, 41076050) and New Century Excellent Talents in University of China (NCET-12-0182). We are grateful to Dr. Mick van der Wegen and two anonymous reviewers for their constructive comments and suggestions that improved the article.

References

Bulletin of China River Sediment (BCRS), 2010. Press of Ministry of Water Resources of the People's Republic of China. http://www.cjh.com.cn/.
Bulletin of China River Sediment (BCRS), 2011. Press of Ministry of Water Resources of the People's Republic of China. http://www.cjh.com.cn/.
Blott, S.J., Pye, K., van der Wal, D., Neal, A., 2006. Long-term morphological change and its causes in the Mersey Estuary, NW England. Geomorphology 81, 185–206.
Brizga, S.O., Finlayson, B.L., 1994. Interactions between upland catchment and lowland rivers: an applied Australian case study. Geomorphology 9, 189–201.
Chen, J.Y., Zhu, H.F., Dong, Y.F., Sun, J.M., 1985. Development of the Changjiang estuary and its submerged delta. Continental Shelf Research 4 (1/2), 47–56.
Chen, Z.Y., Wang, Z.H., Finlayson, B., Chen, J., Yin, D.W., 2010. Implications of flow control by the Three Gorges Dam on sediment and channel dynamics of the middle Yangtze (Changjiang) River, China. Geology 38 (11), 1043–1046.
Chu, Z.X., Zhai, S.K., Lu, X.X., Liu, J.P., Xu, J.X., Xu, K.H., 2009. A quantitative assessment of human impacts on decrease in sediment flux from major Chinese rivers entering the western Pacific Ocean. Geophysical Research Letters 36 (19). http://dx.doi.org/10.1029/2009GL039513.
Dai, S.B., Lu, X.X., 2010. Sediment deposition and erosion during the extreme flood events in the middle and lower reaches of the Yangtze River. Quaternary International 226, 4–11.
Dai, Z.J., Liu, J.T., Xie, H.L., Shi, W.Y., 2012. Sedimentation in the outer Hangzhou Bay, China: the influence of Changjiang sediment load. Journal of Coastal Research. http://dx.doi.org/10.2112/JCOASTRES-D-12-00164.1.
Dai, Z.J., Liu, J.T., Fu, G., Xie, H.L., 2013a. A thirteen-year record of bathymetric changes in the North Passage, Changjiang (Yangtze) estuary. Geomorphology 187, 101–107.
Dai, Z.J., Chu, A., Li, W.H., Li, J.F., Wu, H.L., 2013b. Has suspended sediment concentration near the mouth bar of the Yangtze (Changjiang) estuary been declining in recent years? Journal of Coastal Research 29 (4), 809–818.
Dai, Z.J., James, T.L., Wei, W., 2014. Detection of the Three Gorges Dam influence on the Changjiang (Yangtze River) submerged delta. Scientific Reports 4, 6600. http://dx.doi.org/10.1038/srep06600.
Dyer, K.R., 1997. Estuaries: a Physical Introduction, second ed. John Wiley and Sons, Inc, p. 195.
Emery, W.J., Thomson, R.E., 2001. Data Analysis Methods in Physical Oceanography, second ed. Elsevier, Amsterdam, p. 638.
Evans, G., 2012. Deltas: the fertile dustbins of the continents. Proceedings of the Geologists' Association 123, 397–418.
Fan, Q.J., Gao, M., 2009. Improvement project of deep-draft channel of Yangtze Estuary. Yangtze River 40 (8), 25–30 (in Chinese with English abstract).
Fan, Z.Y., Ge, J.Z., Ding, P.X., Pan, L.Z., 2012. Effect of the deep waterway project on the salinities in the north passage of the Changjiang Estuary. Journal of East China Normal Univerisity (Natural Science) 4, 181–189 (in Chinese with English abstract).
Gagliano, S.M., Meyer-Arendt, K.J., Wicker, K.M., 1981. Land loss on the Mississippi river deltaic plain. Gulf Coast Association Geological Society Transactions 31, 295–300.
Gong, C.L., Yun, C.X., Yu, Z.Y., 2003. Bed-load movement in the south channel and its effect on the south and north passages in the Yangtze Estuary. The Ocean Engineering 21 (3), 62–67.
Gong, W.P., Wang, Y.P., Jia, J.J., 2012. The effect of interacting downstream branches on saltwater intrusion in the Modaomen Estuary, China. Journal of Asian Earth Sciences 45 (2), 223–238.
Gullén, J., Palanques, A., 1997. A historical perspective of the morphological evolution in the lower Ebro River. Environmental Geology 30, 174–180.
Ibe, A.C., 1996. The Niger Delta and sea-level rise. In: Milliman, J.D., Haq, B.U. (Eds.), Sea-level Rise and Coastal Subsidence. Kluwer Academic Publishers, Netherlands, pp. 249–267.
Inman, D.L., Jenkins, S.A., 1984. The Nile littoral cell and man's impact on the coastal zone of the South East Mediterranean. In: 19th Coastal Engineering Conference. Proceedings American Society of Civil Engineers, Houston, Texas, pp. 1600–1617.
Jaffe, B.E., Smith, R.E., Foxgrover, A.C., 2007. Anthropogenic influence on sedimentation and intertidal mudflat change in San Pablo Bay, California: 1856–1983. Estuarine, Coastal and Shelf Science 73, 175–187.
Jiang, C.J., Li, J.F., de Swart, H.E., 2012. Effects of navigational works on morphological changes in the bar area of the Yangtze Estuary. Geomorphology 139–140, 205–219.
Kao, S.J., Milliman, J.D., 2008. Water and sediment discharges from small mountainous rivers, Taiwan: the roles of lithology, episodic events, and human activities. Journal of Geology 116 (5), 431–448.
Lane, A., 2004. Bathymetric evolution of the Mersey Estuary, UK, 106-1997: causes and effects. Estuarine, Coastal and Shelf Science 59, 249–263.
Li, J.F., 1993. The bedload movement in the Changjiang estuary. China Ocean Engineering 7 (4), 441–450.
Li, J.F., Wan, X.N., Ying, M., Zuo, S.H., Fu, G., 2006. Study on the formation and evolution of Jiuduan shoal in the Changjiang estuary. Journal of Sediment Research 6, 44–49 (in Chinese with English abstract).
Li, J.F., Dai, Z.J., Ying, M., Wu, R.R., Fu, G., Xu, H.G., 2007. Analysis on the development and evolution of tidal flats and reclamation of land resource along shore of Shanghai city. Journal of Natural Resources 22 (3), 361–371 (in Chinese with English abstract).
Li, J.F., Dai, Z.J., Liu, X.C., Zhao, J.C., Feng, L.X., 2010. Research on the movement of water and suspended sediment and sedimentation in Nanhui spit of the Yangtze estuary before and after the cdonstruction of reclamation projects on the tidal flat. Journal of Sediment Research 3, 31–37 (in Chinese with English abstract).
Li, P., Yang, S.L., Milliman, J.D., Xu, K.H., Qin, W.H., Wu, C.S., Chen, Y.P., Shi, B.W., 2012. Spatial, temporal, and human-induced variations in suspended sediment concentration in the surface waters of the Yangtze Estuary and adjacent coastal areas. Estuaries and Coasts 35 (5), 1316–1327.
Liu, J.T., Lin, H.L., 2004. Sediment dynamics in a submarine canyon: a case of river-sea interaction. Marine Geology 207, 55–81.
Liu, J.T., Huang, J.S., Hsu, R.T., Chyan, J.M., 2000. The coastal depositional system of a small mountainous river: a perspective from grain-size distributions. Marine Geology 165, 63–86.
Liu, J.P., Xu, K.H., Li, A.C., Milliman, J.D., Velozzi, D.M., Xiao, S.B., Yang, Z.S., 2007. Flux and fate of Yangtze River sediment delivered to the East China Sea. Geomorphology 85 (3–4), 208–224.
Liu, J., Zhao, D.T., Cheng, H.F., 2010. Recent morphological evolution of Jiuduan Shoal and its effect on navigation channel sedimentation of North Passage. Journal of Yangtze River Scientific Research Institute 27 (7), 1–5 (in Chinese with English abstract).
Milliman, J.D., Farnsworth, K.L., 2011. River Discharge to the Coastal Ocean—a Global Synthesis. Cambridge University Press, Cambridge, UK, p. 392.
Milliman, J.D., Shen, H.T., Yang, Z.S., Meade, R.H., 1985. Transport and deposition of river sediment in the Changjiang estuary and adjacent continental shelf. Continental Shelf Research 4 (1/2), 37–45.
Phillips, J.D., 2003. Alluvial storage and the long-term stability of sediment yields. Basin Research 15, 153–163.
Phillips, J.D., Slattery, M.C., 2006. Sediment storage, sea level, and sediment delivery to the ocean by coastal plain rivers. Progress in Physical Geography 30 (4), 513–530.
Phillips, J.D., Slattery, M.C., Musselman, Z.A., 2004. Dam-to-delta sediment inputs and storage in the lower Trinity River, Texas. Geomorphology 62, 17–34.

Pitt, J., 2001. Can we restore the Colorado River delta? Journal of Arid Environments 49, 211–220.
Simmons, H.B., 1955. Some effects of upland discharge on estuarine hydraulics, 1955. Separate Paper No. 792. In: Proceedings ASCE, vol. 81. ASCE Press, Reston, VA.
Spearman, J.R., Dearnale, M.P., Dennis, J.M., 1998. A simulation of estuary response to training wall construction using a regime approach. Coastal Engineering 33, 71–89.
Syvitski, J.P.M., Vörösmarty, C.J., Kettner, A.J., Green, P., 2005. Impact of humans on the flux of terrestrial sediment to the global coastal ocean. Science 308, 376–380.
Syvitski, J.P.M., Kettner, A.J., Hannon, M.T., Hutton, E.W.H., Overeem, I., Brakenridge, G.R., Day, J., Vörösmarty, C., Saito, Y., Giosan, L., Nicholls, R.J., 2009. Sinking deltas. Nature Geoscience 2, 681–689.
Thomas, C.G., Spearman, J.R., Turnbull, M.J., 2002. Historical morphological change in the Mersey estuary. Continental Shelf Research 22, 1775–1794.
Van der Wal, D., Pye, K., Neal, A., 2002. Long-term morphological change in the Ribble Estuary, northwest England. Marine Geology 189, 249–266.
Van der Wegen, M., Roelvink, J.A., 2008. Long-term morphodynamic evolution of a tidal embayment using a two-dimensional, process-based model. Journal of Geophysical Research 113, C03016. http://dx.doi.org/10.1029/2006JC003983.
Van Landeghem, K.J.J., Uehara, K., Wheeler, A.J., Mitchell, N.C., Scourse, J.D., 2009. Post-glacial sediment dynamics in the Irish Sea and sediment dynamics in the Irish Sea and sediment wave morphology: data-model comparisions. Continental Shelf Research 29, 1723–1736.
Wallace, J.W., Dickinson, 1972. Empirical orthogonal representation of time series in the frequency domain, part 1: theoretical consideration. Journal of Applied Meteorology 11, 887–892.
Walling, D.E., Fang, D., 2003. Recent trends in the suspended sediment loads of the world rivers. Global and Planetary Change 39, 111–126.
Wang, J., Bai, S.B., Liu, P., Li, Y.Y., Gao, Z.G., Qu, G.X., Gao, G.G., 2009. Channel sedimentation and erosion of the Jiangsu reach of the Yangtze River during the last 44 years. Earth Surface Processes and Landforms 34, 1587–1593.
Wang, Y.H., Dong, P., Oguchi, T., Chen, S.L., Shen, H.T., 2013. Long-term (1842–2006) morphological change and equilibrium state of the Changjiang (Yangtze) Estuary, China. Continental Shelf Research 56, 71–81.
Yang, S.L., He, S.L., Xie, W.H., 1998. The formation and evolution of the Jiudusha tidal island as well as their relation to the development of the North and South passages in the Yangtze river estuary. The Ocean Engineering 16 (4), 55–64 (in Chinese with English abstract).
Yang, S.L., Zhang, J., Xu, X.J., 2007. Influence of the Three Gorges Dam on downstream delivery of sediment and its environmental implications, Yangtze River. Geophysical Research Letters 34, L10401. http://dx.doi.org/10.1029/2007GL029472.
Yang, S.L., Milliman, J.D., Li, P., Xu, K., 2011. 50,000 dams later: erosion of the Yangtze River and its delta. Global and Planetary Change 75, 14–20.
Yun, C.X., 2004. Evolutionary Rules of the Changjiang Estuary in Recent Decades. China Ocean Press, Beijing (ISBN: 750276219).
Zhou, C.X., 1983. On Sandwave in Yawosha Channel of the Yangtze Estuary. In: Proceedings of the Second International Symposium on River Sedimentation. Water Resources and Electric Power Press, Beijing, pp. 650–661 (in Chinese).